

# Peripapillary intrachoroidal cavitation at the crossroads of peripapillary myopic changes

Adèle Ehongo<sup>1</sup>, Zaki Hasnaoui<sup>1</sup>, Nacima Kisma<sup>1</sup>, Yassir Alaoui Mhammedi<sup>1</sup>, Artemise Dugauquier<sup>1</sup>, Kevin Coppens<sup>2</sup>, Eloïse Wellens<sup>3</sup>, Viviane de Maertelaere<sup>4</sup>, Françoise Bremer<sup>1</sup>, Karelle Leroy<sup>5</sup>

<sup>1</sup>Hôpital Erasme, Bruxelles 1070, Belgium

<sup>2</sup>Cosma Consulting Sijssesdreef 13, Enghien 7850, Belgium

<sup>3</sup>Université Libre de Bruxelles, Bruxelles 1070, Belgium

<sup>4</sup>Biostatistics, IRIBHM Université Libre de Bruxelles, Bruxelles 1070, Belgium

<sup>5</sup>Laboratory of Histology, Université Libre de Bruxelles, Bruxelles 1070, Belgium

**Correspondence to:** Adèle Ehongo. Ophthalmology Department, Erasmus Hospital, route de Lennik 808, Brussels 1070, Belgium. adele.ehongo@erasme.ulb.ac.be

Received: 2022-05-06 Accepted: 2023-09-14

## Abstract

• **AIM:** To analyze the prevalence of peripapillary intrachoroidal cavitation (PICC) in eyes with gamma peripapillary atrophy (γPPA), in eyes with peripapillary staphyloma (PPS) and in those combining γPPA and PPS and to analyze border tissue discontinuity in PICC.

• **METHODS:** This prospective cross-sectional non interventional study included highly myopic eyes. Non-highly myopic eyes were used as control. Radial and linear scans centered on the optic nerve head were performed using spectral-domain optical coherence tomography. Variables were analyzed along the twelve hourly optical coherence tomography sections in both eyes of each subject.

• **RESULTS:** A total of 667 eyes of 334 subjects were included: 229 (34.3%) highly myopic eyes and 438 (65.7%) non highly myopic eyes. The mean age of the highly myopic group was 48.99±17.81y. PICC was found in a total of 40 eyes and in 13.2% (29/220) of highly myopic eyes. PICC was found in 10.4% (40/386) of eyes with γPPA, in 20.5% (40/195) of eyes with PPS and in 22.7% (40/176) of those combining γPPA and PPS. All the eyes with PICC showed the co-existence of γPPA and PPS whereas none of the eyes presenting only one of these entities exhibited PICC. A border tissue discontinuity in the γPPA area was found in all eyes with PICC.

• **CONCLUSION:** We confirm the presence of a border tissue discontinuity in the γPPA area of all eyes with PICC. These findings suggest the involvement of mechanical

factors in the pathogenesis of PICC which may contribute to PICC-related visual field defects.

• **KEYWORDS:** myopia; peripapillary intrachoroidal cavitation; peripapillary staphyloma; gamma peripapillary atrophy; border tissue; myopic complications

**DOI:**10.18240/ijo.2023.12.20

**Citation:** Ehongo A, Hasnaoui Z, Kisma N, Alaoui Mhammedi Y, Dugauquier A, Coppens K, Wellens E, de Maertelaere V, Bremer F, Leroy K. Peripapillary intrachoroidal cavitation at the crossroads of peripapillary myopic changes. *Int J Ophthalmol* 2023;16(12): 2063-2070

## INTRODUCTION

Peripapillary intrachoroidal cavitation (PICC) appears on the fundus as a yellow-orange lesion located at the outer limit of the myopic conus<sup>[1-2]</sup>. Optical coherence tomography (OCT) highlighted the intrachoroidal localization of PICC, which earned it its current name<sup>[1]</sup>. The prevalence of PICC ranges between 2.2% for all myopic thresholds combined to 22% for high myopia<sup>[3]</sup>. In highly myopic eyes, it is lower when screening is done in fundus photographs<sup>[4]</sup> rather than using OCT<sup>[2-3]</sup>.

PICC is associated with glaucoma-like visual field defects<sup>[5]</sup> while glaucoma is correlated with high myopia<sup>[6]</sup>. This co-occurrence is a major cause of diagnostic uncertainty.

Although PICC is consistently located at the outer border of gamma peripapillary atrophy (γPPA; the main histological and OCT characteristic of the myopic conus)<sup>[7-9]</sup>, the prevalence of PICC in eyes with γPPA is not reported to date.

PICC is also associated with peripapillary staphyloma (PPS) at the edge of which the choroid exhibits re-thickening towards the optic nerve head following thinning<sup>[10-11]</sup>. Despite this association, the prevalence of PICC in eyes with PPS is poorly reported<sup>[10]</sup>.

Thus, γPPA and PPS are associated with PICC<sup>[1-2]</sup>. Moreover, they are both suggested in the pathogenesis of PICC<sup>[1,12]</sup>, and they commonly coexist in high myopia. However, the prevalence of PICC in eyes combining γPPA and PPS is unknown so far.

We therefore aimed to contribute to the understanding of the

pathogenesis of PICC by determining its prevalence in eyes with  $\gamma$ PPA, PPS and those combining these entities. We also investigated the border tissue discontinuity which has been mentioned in the pathogenesis of PICC<sup>[1,12]</sup>.

## SUBJECTS AND METHODS

**Ethical Approval** This monocentric cross-sectional observational study was approved by the Ethics Committee of Erasmus Hospital (Brussels, Belgium; Ref: A2019/138), and was conducted in accordance with the ethical principles of the Declaration of Helsinki. Informed and written consent was obtained from all the participants.

**Participants** Subjects aged at least 18y were recruited over 12mo. Participants were approached during their routine visit in our department and through various information channels. Subjects with a history of ocular trauma or posterior segment surgery were excluded.

Considering PICC's prevalence of 17%-22%<sup>[2-3]</sup>, we set the minimum number of highly myopic eyes to 100 to include at least 20 PICCs. For each of the other refractive groups, we recruited at least 50 subjects. Spherical equivalent (SE) refractive thresholds for each group were set according to the World Health Organization International Classification of Diseases<sup>[13]</sup>. Briefly, the SE for each group were as follows. High myopia:  $SE \leq -6$ ; Low myopia:  $-6 < SE \leq -0.5$ ; Non-myopia:  $SE > -0.5$ . Eyes with axial length (AL)  $\geq 26.5$  mm were classified as highly myopic. Additionally, all operated eyes whose preoperative refraction was unknown were only included if  $AL \geq 26.5$  mm and were classified as highly myopic. Finally, 334 subjects (667 eyes) were included.

**Data Collection** For each subject, age, gender, and laterality were recorded. A comprehensive ophthalmic examination was carried out. The SE was measured using Nidek TONOREF2 RKT 2014, Japan and AL was recorded using IOL Master<sup>®</sup> (Carl Zeiss Meditec, Jena, Germany). Color fundus pictures were taken using a VISUCAM<sup>®</sup> non-mydratic camera (PRO NM Carl Zeiss Meditec, Jena, Germany) and the ultra-wide-field HD retinograph Zeiss Clarus<sup>®</sup> 500 (Carl Zeiss Meditec, Jena, Germany). Spectral domain-OCT (SD-OCT) imaging was performed using Spectralis<sup>®</sup> HRA-OCT (Heidelberg Engineering GmbH, Heidelberg Germany).

**SD-OCT Imaging Acquisition** Radial sections were obtained using the glaucoma premium edition module. In addition, we performed two sets of at least 49 vertical and horizontal linear scans centered on the optic nerve head. Sections parallel and perpendicular to the main axis of the papillae exhibiting tilted disc were also made. Additional scans supplemented the examination if necessary (*e.g.*, interference with vessel shadow). The scans covered a volume of at least  $15^\circ \times 25^\circ$  and each scan resulted from the average of at least 60 frames. For PPS, the slice acquisition rectangle was enlarged to include

its boundaries if possible. For spindle papillae, simple radial sections were also made.

**Variables Studied on SD-OCT** Based on established criteria, the diagnosis of PICC<sup>[1,12]</sup>,  $\gamma$ PPA<sup>[7-9]</sup>, and PPS<sup>[10-11]</sup> was made using radial sections and was confirmed by linear OCT scans. We included slight form of PPS<sup>[14]</sup> (Figure 1).

BT configuration was identified as previously defined<sup>[7]</sup>. The diagnosis of BT discontinuity in  $\gamma$ PPA area was based on the interruption of its reflectance<sup>[12]</sup> which had to be detected on at least 2 different sections, or on a full thickness defect at the junction between the conus and the edge of the PICC<sup>[12]</sup>. Finally, we calculated the disc ovality index (OI), an indicator of optic disc tilt<sup>[15]</sup> as the ratio of minimum to maximum disc diameters, using the caliper provided by Spectralis<sup>®</sup>. OI is reported to be low when it is  $\leq 0.8$ .

**OCT Imaging Analysis** The commercialized glaucoma premium edition OCT module provides 24 radial scans centered on the optic disc, totaling 48 spokes. From the 12 o'clock position, every fourth spoke, corresponding to the twelve hourly positions, was analyzed. In case of doubt about the interpretation of a variable on a spoke, reading each of the neighboring spokes helped to clarify it. If the doubt persisted, that variable was deemed as undefined.

OCT variables were analyzed by the first author (Ehongo A). The results were reviewed independently by one of two investigators (Hasnaoui Z and Wellens E). The validated results were then recorded in an Excel spreadsheet. In case of disagreement, the reading was redone collegially. If no consensus was reached, the variable was classified as undefined. All undefined data were excluded from statistical analysis to avoid any bias. After verification of transcription errors, the Excel sheet was submitted to the statistician.

**Statistical Analysis** Statistical analyses were conducted with Excel and R. The study population characteristics were described by means, standard deviations (SD) and intervals for continuous variables and in terms of frequencies, proportions, and percentages for discrete variables. The comparisons of means were made with an unpaired Student's *t*-test and those of percentages with Chi-squared test. Correlations were assessed by the Chi-squared test of independence. The effect of age was studied with a logistic regression and the Wald test. A *P*-value of  $< 0.05$  was considered significant.

## RESULTS

**Characteristics of the Population** A total of 667 eyes of 334 subjects were included: 229 (34.3%) highly myopic eyes and 438 (65.7%) non highly myopic eyes. There were 131 (39.2%) men. The participants' mean age was  $49.7 \pm 18$ y (range: 18-91y). General and ocular characteristics by refraction group and according to the presence or absence of PICC in OCT are summarized in Table 1.

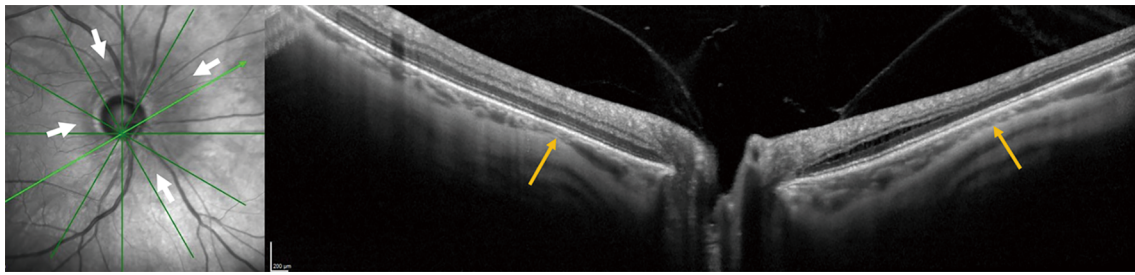


**Figure 1** OCT features of a mild stage peripapillary staphyloma The infra-red image discloses a hyporeflective (white arrows) zone around the papilla. On either side of the optic nerve, the radial OCT section discloses an anterior deformation of the posterior wall of the choroid (orange arrow) in front of which the choroid is thinned. Then the choroid re-thickens towards the optic nerve. OCT: Optical coherence tomography.

**Table 1** Characteristics by refractive group and according to the presence or not of PICC in OCT mean±SD (range)

Parameters	Refractive group (n=667)				P <sup>a</sup>	PICC in OCT (n=657)		P <sup>b</sup>
	High myopia	Low myopia	Non myopia	Non-high myopia		PICC	Non-PICC	
Eye, n (%)	229 (34.33)	212 (31.78)	226 (33.88)	438 (65.67)	-	40 (6.1)	617 (93.9)	-
Age (y)	48.99±17.81 (18-83)	47.57±19.08 (19-91)	52.54±16.86 (21-87)	50.13±18.12 (19-91)	0.437	59.60±17.04 (19-86)	49.11±17.91 (18-91)	<0.001
AL (mm)	27.07±1.41 (24.36-34.31)	24.58±0.80 (22.56-25.95)	23.33±0.81 (21.19-25.58)	23.93±1.08 (21.19-25.95)	<0.001	26.74±2.22 (22.95-32.19)	24.83±1.71 (21.19-30.92)	<0.001
RE (D)	-8.48±4.16 (-30 to -1.62)	-2.73±1.55 (-5.67 to -0.5)	1.08±1.42 (-0.37 to 7.62)	-0.7±2.37 (-5.67 to 7.62)	<0.001	-7.20±5.79 (-21.5 to 1.75)	-2.92±4.26 (-17.12 to 7.62)	<0.001
OI	0.8±0.13 (0.38-1)	0.86±0.10 (0.49-1)	0.89±0.07 (0.58-1)	0.87±0.09 (0.49-1)	<0.001	0.69±0.16 (0.38-0.94)	0.86±0.09 (0.47-1)	<0.001

AL: Axial length; SD: Standard deviation; SE: Spherical equivalent; RE: Refractive error; D: Diopter; OI: Ovality index (min/max axis ratio); Non-high myopia: All the eyes of the sample except highly myopic eyes; PICC: Group of peripapillary intrachoroidal cavitation; Non-PICC: The rest of the study group except PICC; <sup>a</sup>P: Differences between highly myopic eyes and non-highly myopic eyes by Student's *t*-test; <sup>b</sup>P: Differences between PICC group and the rest of the study group by Student's *t*-test.

**Table 2** Proportion of subjects according to the presence or not of high myopia n=667, n (%)

Parameters	Undefined	Present	High myopia (n=229)	Non-high myopia (n=438)	P
γPPA	33/667 (5.0)	388/634 (61.2)	198/219 (90.4)	190/415 (45.8)	<0.001
PPS	21/667 (3.1)	198/646 (30.6)	124/216 (57.4)	74/430 (17.2)	<0.001
PICC	10/667 (1.5)	40/657 (6.1)	29/220 (13.2)	11/437 (2.5)	<0.001

γPPA: Gamma peripapillary atrophy; PPS: Peripapillary staphyloma; PICC: Peripapillary intrachoroidal cavitation; Non-high myopia: The overall sample except eyes with high myopia; P: Differences between the group of high myopic eyes and the rest of the study sample by Chi-squared test.

**Gamma Peripapillary Atrophy** In its reference sample, γPPA was found in 61.2% (388/634) of eyes and its proportion was significantly different between highly 90.4% (198/219) and non-highly 45.8% (190/415) myopic eyes (*P*<0.001; Table 2). Among the eyes with γPPA, 10.4% (40/386) had PICC (Table 3, Figure 2).

**Peripapillary Staphyloma** In its reference sample, PPS was detected in 30.6% (198/646) of eyes. Its proportion was significantly different between highly 57.4% (124/216) and non-highly 17.2% (74/430) myopic eyes (*P*<0.001; Table 2). Of all eyes with PPS, 20.5% (40/195) had PICC (Figure 2, Table 3).

**Border Tissue** In the reference sample for border tissue obliquity, its external configuration was observed in 64.7% (390/603) of all eyes (Table 3). This proportion was 100% in eyes with PICC, which is significantly different from that 62.2% (350/563) in non-PICC eyes (*P*<0.001). In the reference sample for border tissue discontinuity, it was found in 6.4%

(42/655) of all eyes, and in 100% of eyes with PICC, which was significantly different from that 0.3% (2/615) in eyes without PICC (*P*<0.001; Table 3).

**Peripapillary Intrachoroidal Cavitation** Forty eyes (6.1%, 40/657) of 33 subjects, including 19 women (57.6%) had PICC (Figures 3 and 4). Twenty-three left eyes had PICC (57.5%), and 7 subjects had PICC in both eyes (21.2%). The mean age, AL, refractive error and OI of eyes with and without PICC were significantly different (Table 1). The number of PICC per decade increased from 30 to 70y, then decreased (Figure 5). Logistic regression analysis showed an association between age and PICC (*P*=0.014). The proportion of PICC in highly myopic eyes 13.2% (29/220) was significantly different to that 2.5% (11/437) of non-highly myopic eyes (*P*<0.001; Table 2). The proportion of low OI (OI≤0.8) was significantly different between the groups with 72.5% (29/40) and without 23.3% (144/617) PICC (*P*<0.001; Table 3).

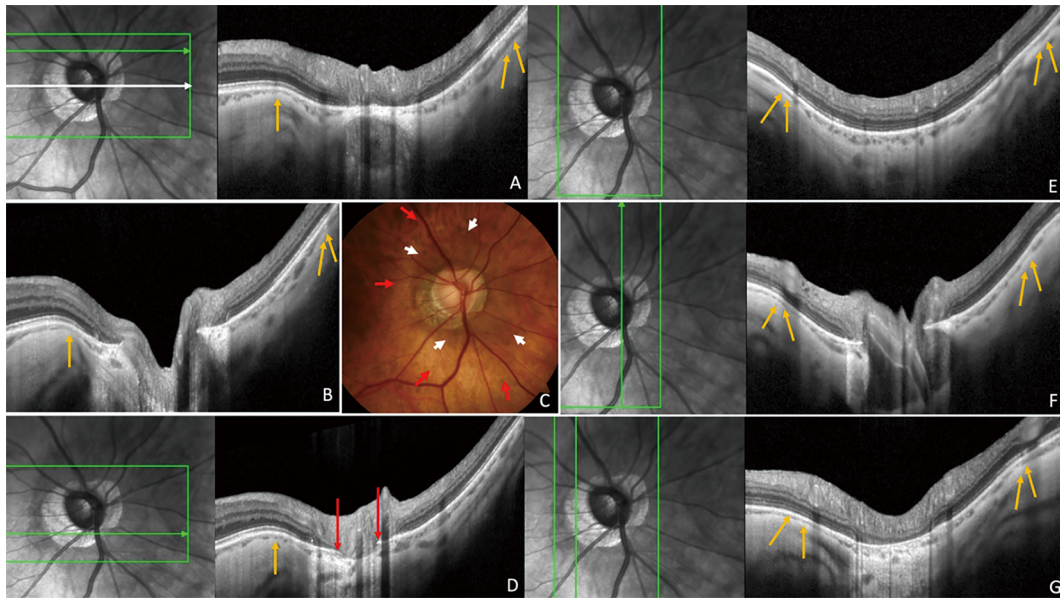


**Figure 2** Fundus image and OCT features of a right myopic eye presenting gamma peripapillary atrophy ( $\gamma$ PPA) and peripapillary staphyloma (PPS) without PICC A, B, D: Horizontal OCT slices along the green (A, D) and white (B) arrows in the infra-red images. On the temporal side, the choroid is thinned along the anterior protrusion of the curvature of the eye (orange arrow) and thicker on either side of it. On the nasal side, due to the steeper slope of the wall of the eye, the change in curvature is slighter (double orange arrows). The  $\gamma$ PPA is the area devoid of Bruch's membrane between the red arrows (D). C: Fundus image. PPS is characterized by a dark area (white arrows) around the papilla, itself surrounded by a lighter area (red arrows). E, F, G: Vertical slices along the green arrow of each corresponding infra-red image. The pair of orange arrows show the anterior distortion of the curvature of the posterior choroidal wall along which the choroid is thinned whereas it is less thin on either side of this anterior deformation.

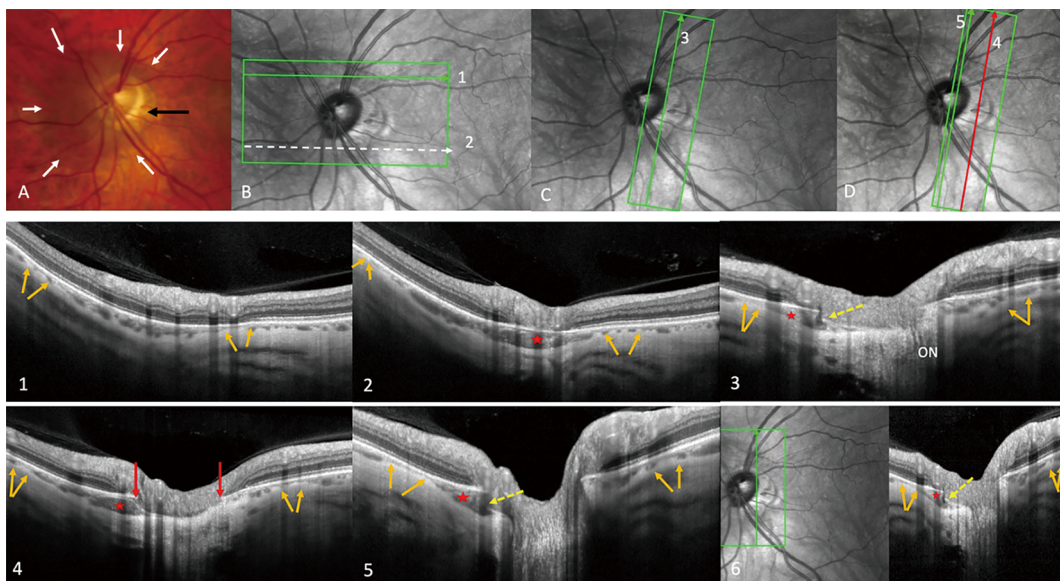


**Figure 3** Fundus image and OCT sections of a peripapillary intrachoroidal cavitation (PICC) The combined presence of gamma peripapillary atrophy ( $\gamma$ PPA) and peripapillary staphyloma (PPS) is disclosed A: Color image of the fundus in a left eye. PICC located at the inferior border of the conus is not obvious in this fundus. The white arrows outline the limits of the dark area of the PPS. The more peripheral pale area of the PPS is inconspicuous in this case. Black arrow: myopic conus. B-D: Infrared OCT images. Each arrow in these images indicates the location and orientation of OCT section displaying the same number. In each OCT section, the pair of orange arrows show a thinning of the choroid between two less thinned areas, hallmark of PPS. Horizontal sections. Section 1 is located on the upper peripapillary (PP) zone and section 2 on the lower PP zone, through the PICC (red star). Oblique-vertical sections. Section 3 intercepts both the optic nerve (ON) and the  $\gamma$ PPA. Section 4 runs across the PP area and discloses, the zone devoid of Bruch's membrane (between the red arrows), called  $\gamma$ PPA. Sections 5 & 6 run across the optic nerve head and the PICC. The PICC (red star) is visible in slices 2 to 6. The border tissue presents an interruption of its reflectivity (dashed yellow arrows) on sections 3, 5 & 6. Comparing slices 1 (out of the PICC, upper PP area) and 2 (through the PICC, lower PP area), the bowing of the posterior choroidal wall (between the orange arrows), visible in both cases is pronounced in slice 2 which reveals the PICC.



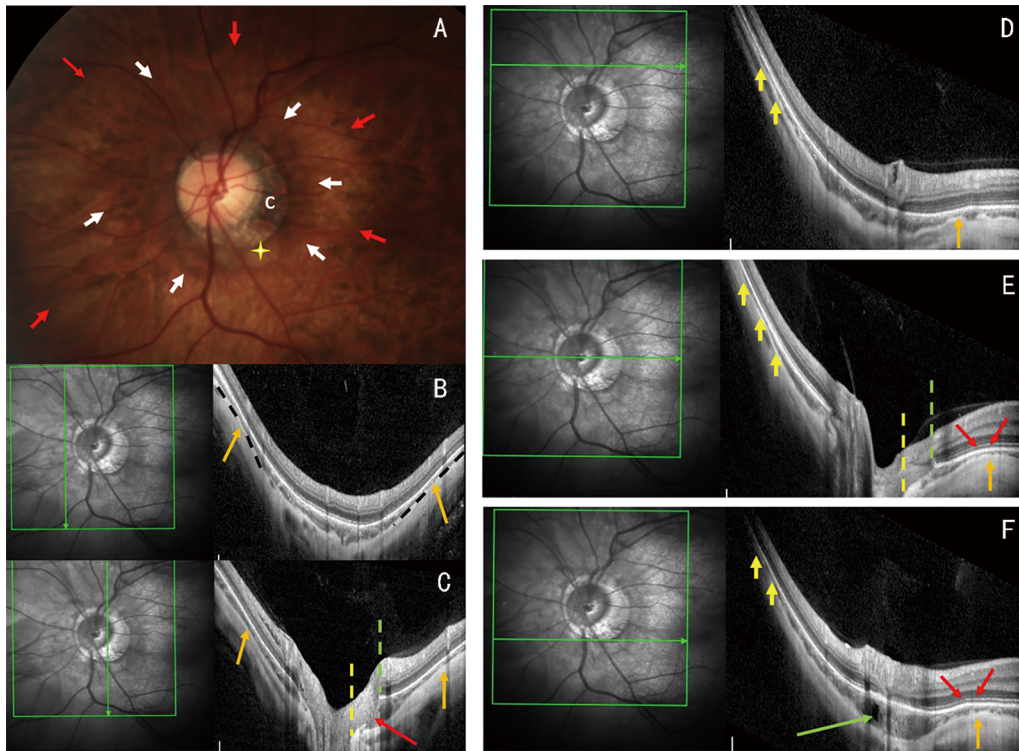


**Figure 4** Fundus image and OCT scans of a peripapillary intrachoroidal cavitation (PICC) The coexistence of gamma peripapillary atrophy ( $\gamma$ PPA) and peripapillary staphyloma (PPS) is shown in this left eye with an axial length of 31.0 mm. A: Color fundus image. The PPS appears as a dark peripapillary (PP) area (white arrows) surrounded by a lighter colored area (red arrows). The yellow cross shows the PICC located at the lower margin of the conus (c). B-F: The green arrow in each infrared OCT image indicates the location and orientation of the section on the right. B-C: Vertical sections. Section B is through the nasal PP area. The orange arrows show the pinching of the choroid (thinning between 2 less thin areas) on the edge of the PPS. Section C intercepts both the optic nerve head and PICC and shows the border tissue discontinuity (red arrow). In both sections, between the left and right orange arrows, the radius of curvature of the eye is lesser than that of the neighboring area and the choroid is thickened toward the posterior pole. D-F: Horizontal sections. Sections D and E pass across the superior PP zone and the optic nerve head respectively. Section F intercepts the lower PP zone and the PICC which presents a hypo-reflective cyst (green arrow). Temporal edge of the PPS. The red arrows in sections E and F, show the anterior distortion of the curvature of the eye corresponding to the temporal edge of the PPS, followed by its posterior protrusion toward the posterior pole. The choroid, which is thin along the anterior distortion (orange arrows) widens on either side of it. Nasal edge of the PPS. On horizontal sections D to F. Due to the steep curvature of the wall of the eye related to the axial length, the nasal edge of the PPS is indistinct (yellow arrows). In this nasal part, the upper and lower limits of the PPS are nevertheless detected by a slight change in curvature underlined by the dotted black line on the vertical section B (orange arrows).  $\gamma$ PPA: On sections C and E, it is between the edge of the optic nerve head (dashed yellow line) and the Bruch's membrane (dashed green line). Posterior choroidal wall. Comparing slices D (outside the PICC) and F (through the PICC), both the anterior and posterior deformities of the choroidal wall are pronounced in section F.

**Table 3** Cross-presence of PICC with other anomalies on OCT

Parameters	PPS	$\gamma$ PPA	BT-EO	BT-Discont	OI $\leq$ 0.8
Undefined	24 (3.6)	35 (5.7)	64 (9.6)	12 (1.8)	10 (1.5)
Reference sample	643	632	603	655	657
Anomalies present	195/643 (30.3)	386/632 (61.1)	390/603 (64.7)	42/655 (6.4)	173/657 (26.3)
PICC in reference sample	40/643 (6.2)	40/632 (6.3)	40/603 (6.6)	40/655 (6.1)	40/657 (6.1)
Coexistence of anomalies and PICC in PICC	40/40 (100)	40/40 (100)	40/40 (100)	40/40 (100)	29/40 (72.5)
PICC in anomalies	40/195 (20.5)	40/386 (10.4)	40/390 (10.3)	40/42 (95.2)	29/173 (16.8)
Non PICC in reference sample	155/643 (24.1)	346/632 (54.8)	350/603 (58)	2/655 (0.3)	144/657 (22)
Anomalies in non-PICC	155/603 (25.7)	346/592 (58.5)	350/563 (62.2)	2/615 (0.3)	144/617 (23.3)
<i>P</i>	<0.001 <sup>a</sup>	<0.001 <sup>a</sup>	<0.001 <sup>a</sup>	<0.001 <sup>b</sup>	<0.001 <sup>a</sup>

$\gamma$ PPA: Gamma peripapillary atrophy; PPS: Peripapillary staphyloma; PICC: Peripapillary intrachoroidal cavitation; BT-EO: External obliquity of border tissue; BT-Discont: Discontinuity of the border tissue; OI: Ovality index; *P*: Differences between the proportions of the entity within the group with PICC and that without PICC. <sup>a</sup>Chi-squared test; <sup>b</sup>Fisher test.

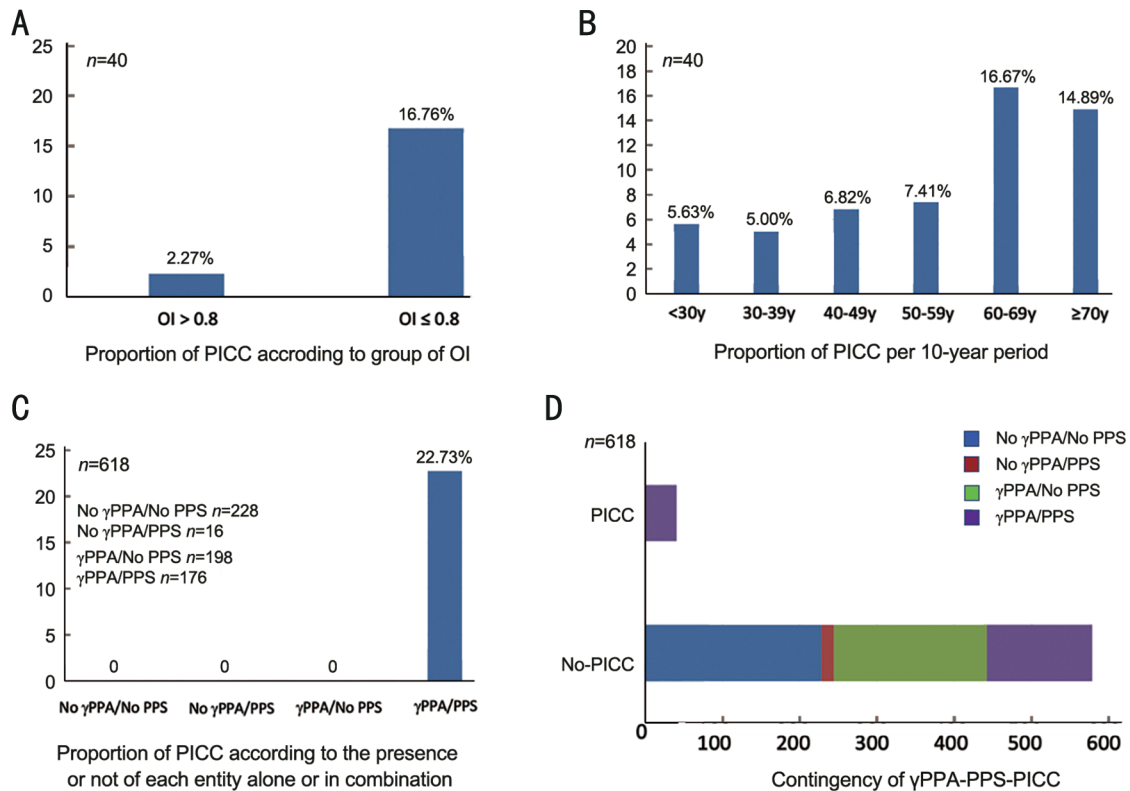


**Figure 5** Proportion of PICC according to ovality index (A), age (B), presence or absence of each entity, alone or in combination (C) and contingency plot of  $\gamma$ PPA-PPS-PICC (D) In cross-analysis (C, D), the data excluded for each variable are cumulative. PICC: Peripapillary intrachoroidal cavitation;  $\gamma$ PPA: Gamma peripapillary atrophy; PPS: Peripapillary staphyloma; OI: Ovality index.

**Analysis of the Coexistence between PICC,  $\gamma$ PPA, and PPS**

In 228 eyes, neither PPS nor  $\gamma$ PPA was found. PPS without  $\gamma$ PPA was detected in 16 eyes while 198 eyes exhibited  $\gamma$ PPA without PPS. The two entities coexisted in 176 eyes, 22.7% (40/176) of which had a PICC. The proportion of PICC in the group combining PPS and  $\gamma$ PPA was significantly different from that in the rest of the study group ( $P < 0.001$ ; Figure 5). The coexistence of PPS and  $\gamma$ PPA was found in all cases of PICC.

**DISCUSSION**

In this study using SD-OCT, the prevalence of PICC in highly myopic eyes was within the reported range<sup>[2-4]</sup> and all eyes with PICC exhibited  $\gamma$ PPA, consistent with previous reports<sup>[7-9]</sup>, as PICC is located at the outer limit of the myopic conus<sup>[1-5,12]</sup>. Finally, the border tissue was externally oblique at the  $\gamma$ PPA area, which is consistent with the literature<sup>[7]</sup>.

PICC was found in 10.4% of eyes with  $\gamma$ PPA whereas it was not found in eyes exhibiting only  $\gamma$ PPA which, is an unprecedented result and suggests that, although necessary, the peripapillary changes associated with  $\gamma$ PPA are not sufficient to have a PICC and that other factors are involved.

We found a significantly lower mean OI in the PICC than in the control eyes, as previously reported<sup>[2]</sup>. Additionally, we found a significantly higher proportion of papillae with low OI ( $\leq 0.8$ ) in the PICC group compared to the control group.

This supports the results of an intra-individual comparison of unilateral cases of PICC<sup>[16]</sup>, and suggests the influence of mechanical factors. The stress undergone by the peripapillary region, underlies one of the pathogenetic hypotheses of the PICC<sup>[12]</sup> suggesting that PICC would be favored by the mechanical phenomena linked to the onset and progression of tilted disc.

Of note, this low OI, could indicate not only the stress experienced by these eyes, but also the risk of functional damage, as low OI is related to visual field defects<sup>[15]</sup>. Studies addressing this issue are awaited.

PICC was not detected in eyes presenting only PPS, which is also a novelty. However, we found PICC in 20.5% of the whole sample of eyes exhibiting PPS, suggesting that the changes related to PPS are not sufficient to lead to PICC. The prevalence of PICC in eyes with PPS in our study was lower than that reported by Shinohara *et al*<sup>[10]</sup>. This discrepancy could be related to the smaller number of eyes in the previous study.

At the edge of each PICC, we observed thinning of the choroid against an anterior protrusion of the wall of the eye, or a gradual thinning of the choroid without a sharp anterior deformation of the wall of the eye. The posterior excursion of the thinned and remodeled myopic<sup>[17]</sup> sclera, inducing choroidal thickening, was previously disclosed in the PICC<sup>[12]</sup> whereas choroidal thinning preceding this thickening has just

been revealed<sup>[18]</sup>. This sequence of choroidal configurations, hallmarks of PPS, testifies to the existence of stresses exerted in the peripapillary region and more pronounced at the level of the PICC, suggesting a local accentuation of the mechanisms involved. Recent studies have suggested these deformations to result from traction of the dura on the sclera during eye movement<sup>[18-19]</sup>.

Thickening of the choroid against the wall of the optic nerve head, in a PPS increases the distance between Bruch's membrane and the sclera at this wall, leading to the other pathogenetic hypothesis according to which this choroidal thickening promotes the occurrence of PICC<sup>[1,20]</sup>. Given this assumption, all PICCs should present a posterior staphyloma, which we observed in our series. Ohno-Matsui *et al*<sup>[21]</sup> also found 100% posterior staphylomas in eyes with temporally located PICCs. This finding therefore deserves to be confirmed, the posterior staphyloma being a criterion of pathologic myopia, which could lead to reconsidering the place of PICC in the pool of myopic complications. In support of its clinical implication, it has recently been shown that PICC is more common in eyes with a higher category of myopic maculopathy<sup>[4]</sup>.

Thus, we found PPS in all eyes with PICC and only 20.5% PICC in eyes with PPS. Furthermore, in the absence of  $\gamma$ PPA, no PICC was detected in eyes with PPS and vice versa, suggesting that, although PPS is necessary, it is not sufficient for the presence of PICC, and that the combination of the two entities is paramount for the presence of PICC. However, only 22.7% of eyes combining these entities had PICC, suggesting that their coexistence, although necessary, is not sufficient for the presence of PICC, the appearance of which most likely also depends on other factors, warranting further investigation.

We found that the prevalence of PICC increases after 30y and that PICC is related to age, consistent with previous works<sup>[4]</sup>. We also found that the mean age of subjects with PICC was higher than that of subjects without PICC. These results support that PICC is an acquired condition and that its onset depends on the interaction of contributing factors and time. Finally, a new observation revealed by our study is that the prevalence of PICC might decrease with aging, which warrants confirmation; Our analysis per period of 10y showed that after an increase in the prevalence of PICC with age, a decrease in its prevalence appeared around the age of 70y. As the prevalence of  $\gamma$ PPA increases with age<sup>[8]</sup>, we therefore suggest that the extension of  $\gamma$ PPA which is accompanied by tissue thinning and atrophy might lead to the progressive involution of some PICCs, and thus to the reduction of the prevalence of PICC with aging.

In our series, 100% of the PICCs exhibited a border tissue discontinuity. Signs of this discontinuity are either the presence

of a communication between the PICC and the vitreous or a simple interruption of the reflectance detected within the hyper-reflective line that characterizes border tissue<sup>[12]</sup>. Border tissue discontinuity could be indicative of mechanical stress involved in its pathogenesis. Our study design does not allow longitudinal monitoring.

Limitations in our study was that monocentricity could constitute a potential recruitment bias.

As image quality in high myopia, the target group, is not always optimal due to tissue alterations, potentially contributing eyes were excluded. Nevertheless, our protocol led us to qualify as undefined any variable presenting ambiguous characteristics, in order to limit biases and to preserve our sample size. This strategy reduced the number of excluded eyes.

The World Health Organization International Classification of Diseases was used to define myopia but, the patients did not receive cycloplegia. Thus, some young patients may present an overestimation of their myopic error by accommodation. Another potential source of refractive error may be the absence of keratometry or corneal topography. Nevertheless, our prevalence of PICC in highly myopic eyes is consistent with previous reports.

In conclusion, PICC was found in 10.4% of eyes with  $\gamma$ PPA and in 20.5% of eyes with PPS. We found that the prevalence of PICC increased with age, and then decreased with aging. We did not find PICC in the eyes exhibiting  $\gamma$ PPA without PPS and vice versa. We observed a combination of  $\gamma$ PPA and PPS in all cases of PICC. However, PICC was only detected in 22.7% of eyes combining these entities, suggesting that changes related to each of them interact over the time to promote PICC occurrence and that other factors are also involved.

We confirm the correlation between PICC and the border tissue discontinuity in the  $\gamma$ PPA area. This discontinuity that we found in all PICCs but not in control eyes suggests the involvement of mechanical factors in the pathogenesis of PICC. The low mean ovality index that we observed in PICCs supports the role of mechanical factors which may contribute to PICC-related VF defects.

Biomechanical and longitudinal studies are expected to clarify the mechanisms involved in the pathogenesis of PICC and their clinical implications.

#### ACKNOWLEDGEMENTS

The authors thank all the technicians of the department who contributed to the data acquisition of this study. In addition, the authors are grateful to Mr. Driss Khayer (Department of Ophthalmology, Erasmus Hospital, Brussels, Belgium) who performed most of the OCT acquisitions.

**Authors' contributions:** Designed the experiment: Ehongo A, de Maertelaer V, Bremer F, Leroy K; Conducted the experiment: Ehongo A, Hasnaoui Z, Kisma N, Alaoui

Mhammedi Y, Dugauquier A, Coppens K, Wellens E; Analyzed/interpreted data: Ehongo A, Hasnaoui Z, Coppens K, de Maertelaer V, Bremer F, Leroy K; Provided materials: Ehongo A, Kisma N, Alaoui Mhammedi Y, Dugauquier A, Wellens E; Wrote the article: Ehongo A; Proofread/revised article: Ehongo A, Hasnaoui Z, Kisma N, Alaoui Mhammedi Y, Dugauquier A, Coppens K, Wellens E, de Maertelaer V, Bremer F, Leroy K.

**Conflicts of Interest: Ehongo A, None; Hasnaoui Z, None; Kisma N, None; Alaoui Mhammedi Y, None; Dugauquier A, None; Coppens K, None; Wellens E, None; de Maertelaer V, None; Bremer F, None; Leroy K, None.**

#### REFERENCES

- Toranzo J, Cohen SY, Erginay A, Gaudric A. Peripapillary intrachoroidal cavitation in myopia. *Am J Ophthalmol* 2005;140(4):731-732.
- You QS, Peng XY, Chen CX, Xu L, Jonas JB. Peripapillary intrachoroidal cavitations. The Beijing Eye Study. *PLoS One* 2013; 8(10):e78743.
- Choudhury F, Meuer SM, Klein R, Wang D, Torres M, Jiang X, McKean-Cowdin R, Varma R; Chinese American Eye Study Group. Prevalence and characteristics of myopic degeneration in an adult Chinese American population: the Chinese American Eye Study. *Am J Ophthalmol* 2018;187:34-42.
- Liu R, Li Z, Xiao O, et al. Characteristics of peripapillary intrachoroidal cavitation in highly myopic eyes: The Zhongshan Ophthalmic Center-Brien Holden Vision Institute High Myopia Cohort Study. *Retina* 2021;41(5):1057-1062.
- Kim J, Kim J, Lee EJ, Kim TW. Parapapillary intrachoroidal cavitation in glaucoma: association with choroidal microvasculature dropout. *Korean J Ophthalmol* 2021;35(1):44-50.
- Ha A, Kim CY, Shim SR, Chang IB, Kim YK. Degree of myopia and glaucoma risk: a dose-response meta-analysis. *Am J Ophthalmol* 2022;236:107-119.
- Wang YX, Panda-Jonas S, Jonas JB. Optic nerve head anatomy in myopia and glaucoma, including parapapillary zones alpha, beta, gamma and delta: histology and clinical features. *Prog Retin Eye Res* 2021;83:100933.
- Guo XX, Chen X, Li SS, Li M, Yang XF, Zhao L, You R, Wang YL. Measurements of the parapapillary atrophy area and other fundus morphological features in high myopia with or without posterior staphyloma and myopic traction maculopathy. *Int J Ophthalmol* 2020;13(8):1272-1280.
- Guo Y, Liu LJ, Tang P, Feng Y, Lv YY, Wu M, Xu L, Jonas JB. Parapapillary gamma zone and progression of myopia in school children: The Beijing Children Eye Study. *Invest Ophthalmol Vis Sci* 2018;59(3):1609-1616.
- Shinohara K, Shimada N, Moriyama M, Yoshida T, Jonas JB, Yoshimura N, Ohno-Matsui K. Posterior staphylomas in pathologic myopia imaged by widefield optical coherence tomography. *Invest Ophthalmol Vis Sci* 2017;58(9):3750-3758.
- Ohno-Matsui K, Wu PC, Yamashiro K, Vutipongsatorn K, Fang Y, Cheung CMG, Lai TYY, Ikuno Y, Cohen SY, Gaudric A, Jonas JB. IMI pathologic myopia. *Invest Ophthalmol Vis Sci* 2021;62(5):5.
- Spaide RF, Akiba M, Ohno-Matsui K. Evaluation of peripapillary intrachoroidal cavitation with swept source and enhanced depth imaging optical coherence tomography. *Retina* 2012;32(6):1037-1044.
- Flitcroft DI, He M, Jonas JB, Jong M, Naidoo K, Ohno-Matsui K, Rahi J, Resnikoff S, Vitale S, Yannuzzi L. IMI--defining and classifying myopia: a proposed set of standards for clinical and epidemiologic studies. *Invest Ophthalmol Vis Sci* 2019;60(3):M20-M30.
- Tanaka N, Shinohara K, Yokoi T, Uramoto K, Takahashi H, Onishi Y, Horie S, Yoshida T, Ohno-Matsui K. Posterior staphylomas and scleral curvature in highly myopic children and adolescents investigated by ultra-widefield optical coherence tomography. *PLoS One* 2019;14(6):e0218107.
- Tay E, Seah SK, Chan SP, Lim AT, Chew SJ, Foster PJ, Aung T. Optic disk ovality as an index of tilt and its relationship to myopia and perimetry. *Am J Ophthalmol* 2005;139(2):247-252.
- Dai Y, Jonas JB, Ling Z, Wang X, Sun X. Unilateral peripapillary intrachoroidal cavitation and optic disk rotation. *Retina* 2015; 35(4):655-659.
- Yu Q, Zhou JB. Scleral remodeling in myopia development. *Int J Ophthalmol* 2022;15(3):510-514.
- Ehongo A, Bacq N, Kisma N, Dugauquier A, Alaoui Mhammedi Y, Coppens K, Bremer F, Leroy K. Analysis of peripapillary intrachoroidal cavitation and myopic peripapillary distortions in polar regions by optical coherence tomography. *Clin Ophthalmol* 2022;16:2617-2629.
- Lee WJ, Kim YJ, Kim JH, Hwang S, Shin SH, Lim HW. Changes in the optic nerve head induced by horizontal eye movements. *PLoS One* 2018;13(9):e0204069.
- Parlak M, Ipek SC, Saatci AO. Peripapillary whitening in high myopia: only a staphyloma posticum? *Ophthalmologie* 2020;117(4):379-383.
- Ohno-Matsui K, Shimada N, Akiba M, Moriyama M, Ishibashi T, Tokoro T. Characteristics of intrachoroidal cavitation located temporal to optic disc in highly myopic eyes. *Eye(Lond)* 2013;27(5):630-638.